Ab initio calculations of low-energy electron scattering by HCN molecules

Ashok Jain* and D. W. Norcross†
Joint Institute for Laboratory Astrophysics, University of Colorado and National Bureau of Standards, Boulder, Colorado 80309
(Received 5 March 1985)

We report results for vibrationally elastic scattering over the energy range 0.0006—11.6 eV. The interaction potential is composed of a near-Hartree-Fock static term plus a parameter-free model of the correlation-polarization potential. The exchange interaction is included exactly through a separable expansion. Results with a model-exchange potential (free-electron-gas plus orthogonalization) are also reported. A resonance appears in Π symmetry near 2.7 eV (width 1.9 eV) that may be the same feature observed in several experiments. In the model-exchange calculation the Π resonance is shifted toward higher energy (3.8 eV, width 2.4 eV). The Σ symmetry was also found to be very sensitive to the treatment of exchange and to the effect of polarization. Differential and rotational excitation cross sections are evaluated in the multipole-extracted adiabatic-nuclei approximation. Results are compared with the available experimental and theoretical data.

I. INTRODUCTION

In recent years there has been a great deal of theoretical work[1] on electron-polar molecule scattering theory. In this paper we investigate a linear polyatomic molecule, HCN, that has a sizable dipole moment [D(expt.)$=1.174$ a.u.]. Previous low-energy calculations for this system are limited to the laboratory-frame close-coupling study of Saha *et al.*[2] in a very small energy region (0.0006—0.1 eV), first Born calculations of Seal,[3] and some illustrative applications of effective range theory by Fabrikant.[4] Saha *et al.* employed the asymptotic forms of the dipole, quadrupole, and polarization interactions, thus completely neglecting short-range effects (including exchange). At higher energies Jain and Tayal[5] studied the *e*-HCN elastic scattering in a two-potential hybrid approach (21.6—700 eV).

A theoretical study of the *e*-HCN system is important for several reasons.

(i) In a CN laser system the presence of HCN is essential in order to produce stimulated emission. Here, a possible pumping mechanism is $HCN + e \rightarrow HCN^* + e$, followed by the predissociation process, $HCN^* \rightarrow H(^1S) + CN(A\,^2\Pi)$.[6]

(ii) HCN is known to exist in comets and the interstellar medium.[7] It has been suggested that, in some interstellar conditions, electron impact on HCN molecules may be significant in addition to the dominant H_2-molecule processes.[8]

(iii) Another point of interest is its large dipole moment, which can support an infinite number of bound states in the fixed-nuclei approximation (in Σ symmetry only), thus affecting the low-energy *e*-HCN cross sections.

Experimental observations of the *e*-HCN collision system are relatively scarce. The only recent published measurements are of differential cross sections, by Srivastava *et al.*,[9] in the range 3—50 eV and from 20° to 130°. In order to obtain absolute numbers, they normalized to simultaneous measurements for helium. Earlier, Tice and Kivelson[10] studied the interaction of polar molecules with very slow electrons by means of the cyclotron resonance; only the momentum-transfer cross section at 0.025 eV is available from their observations. They fit a Born-type formula to their measurements in order to estimate momentum-transfer cross sections at other energies.

At about the same time, Inoue[11] observed dissociative attachment of electrons to HCN, forming CN^- with a probability that peaked around 2.5 eV in electron energy. A peak at 2.26 eV was also observed in total scattering by Burrow,[12] using electron transmission spectroscopy. A resonance at about this energy is expected since HCN is isoelectronic to N_2, which has a well-known Π_g shape resonance at 2.4 eV in electron scattering. It was also observed recently, at about 2.3 eV, in vibrational excitation measurements,[13] the first to provide some experimental confirmation of its symmetry; it appeared in the CN stretch modes, as expected, as well as in the bending modes. Tronc[13] also observed a resonance, interpreted as Σ, at about 6.2 eV exciting primarily the CH stretch modes.

There are also several other experimental studies[14] indicating the existence of a state of HCN^-, which Pacansky *et al.*[15] attempted to interpret by means of a calculated potential-energy surface for HCN^-. They obtained a state with a negative electron affinity (1.95 eV), whose geometry was both bent ($\theta \sim 122°$) and stretched with respect to HCN. While this result has been correctly criticized[16] as not representing the ground state of HCN^-, it may well be consistent with the resonances observed in the electron scattering measurements.[11—13]

In this paper we present differential, integral, and momentum-transfer cross sections from astrophysically important low energies (6×10^{-4} eV) to 11.6 eV for rotationally elastic and inelastic transitions and for total scattering (vibrationally and electronically elastic). We were particularly interested in confirming theoretically the existence and symmetry of the Π resonance. We also wished to explore the possibility of a Σ resonance correlating more directly with the lowest dissociation state, $H + CN^-$.

Since the physical model and computational method have been discussed at length elsewhere recently,[17] only a brief account is given in Sec. II. Full details of the calculations are provided in Sec. III. Section IV contains the results and discussion, and the work is summarized with concluding remarks in Sec. V. We use atomic units throughout this paper unless otherwise specified ($\hbar = m_e = e = 1$, energy in hartrees and length in bohr radii).

II. PHYSICAL MODEL AND COMPUTATIONAL METHOD

The equation for the scattered electron wave function is set up using a single-center integral-equations formulation of the close-coupling approximation.[18] These equations are ideally suited to calculations employing purely local potentials (static and local models of exchange and polarization). They have recently been modified[19] to implement an exact treatment of exchange (through a separable expansion[20]). The integral equations were solved numerically in the molecular body-fixed frame of reference in the fixed-nuclei approximation for the equilibrium (linear) geometry of the HCN molecule, i.e., neglecting the rotational and vibrational Hamiltonians.

A near-Hartree-Fock wave function for the HCN molecule[21] was used for the calculations employing a model-exchange potential.[22] Since this model does not automatically enforce the orthogonality of scattering and bound orbitals of like symmetry that is required for a closed-shell system like HCN, we imposed orthogonality as an additional constraint in some of our calculations.

For the calculations in which exchange was treated exactly, we generated a Gaussian orbital basis (Table I) for the HCN target using a standard molecular structure code[23] and other auxiliary programs.[24] Since this basis was used to expand the exchange kernel, it was necessarily different for each scattering symmetry, but yields the same properties and static electron-molecule interaction potential. The basis sets, with diffuse functions on all centers, were taken to be (H/C/N):

Σ (6*s* 4*p* /10*s* 6*p* 2*d* /10*s* 6*p* 2*d*) [4*s* 4*p* /6*s* 4*p* 2*d* /6*s* 4*p* 2*d*]

Π (6*s* 4*p* /10*s* 6*p* 2*p* 2*d* /10*s* 6*p* 2*p* 2*d*) [4*s* 4*p* /6*s* 4*p* 2*p* 2*d* /6*s* 4*p* 2*p* 2*d*]

Δ (6*s* 4*p* /10*s* 6*p* 2*d* 3*d* /10*s* 6*p* 2*d* 3*d*) [4*s* 4*p* /6*s* 4*p* 2*d* 3*d* /6*s* 4*p* 2*d* 3*d*] ,

where the usual convention (( ) for primitives and [ ] for contracted) has been used to represent the Gaussian-type orbital (GTO) basis. Only the model-exchange potential was employed for higher scattering symmetries. The total energies, dipole and quadrupole moments, and ionization energies (Koopman's theorem) from the two wave functions are given in Table II, along with measured values.

When including polarization effects we used a parameter-free correlation-polarization model.[28] The monopole and quadrupole terms were matched at their crossings to the asymptotic forms $\alpha_0/2r^{-4}$ and $\alpha_2 P_2(\theta)/2r^{-4}$, respectively, using experimental values[29] for α_0 (17.5) and α_2 (9.0). This potential is illustrated for $\lambda = 0$ in Fig. 1, where it can be compared with the static and free-electron-gas model-exchange potentials. The crossing point between the correlation and asymptotic polarization potentials falls within the range 0.9—1.1 eV obtained for several other closed-shell systems.[28]

In order to examine the effects of exchange and polarization in detail, we carried out calculations with several models of the interaction potential: SE, static plus model exchange; SEP, SE plus polarization; SEPO, SEP plus orthogonalization; ESE, exact static exchange; ESEP, ESE plus polarization.

A feature common to all *e*-polar molecule scattering is the problem of proper convergence of scattering parameters, particularly of the total and the differential cross sections (DCS). In addition, if the scattering equations are solved in the molecular body-fixed frame of reference, neglecting all coupling between the incident electron angular momenta and the nuclear motion, the DCS diverges in the forward direction resulting in an undefined integral cross section (the momentum-transfer cross section

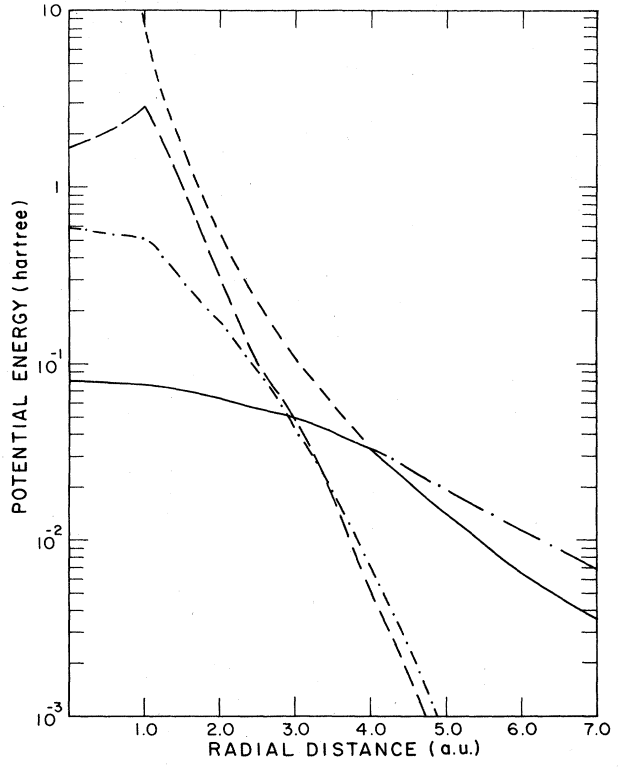

FIG. 1. *e*-HCN interaction potential (for the spherical term only): ———, static potential; —·—·—, free-electron-gas exchange potential; – – – –, polarization term; —·—, correlation-polarization potential beyond the crossing point; ——, correlation-polarization potential.

TABLE I. The primitive Gaussian-type orbital (GTO) basis set plus diffuse functions on all centers of HCN (Σ symmetry).[a]

Center	Type	Exponent	Coefficient
H	s	33.644 40	0.025 374
		5.057 96	0.189 683 0
		1.146 800	0.852 930 3
		0.321 144	1.0
		0.101 309	1.0
		0.032	1.0
	p	1.0	1.0
		0.337 070	1.0
		0.079 830	1.0
		0.024 684	1.0
C	s	4232.6100	0.006 228
		634.8820	0.047 676
		146.0970	0.231 439
		42.4974	0.789 108 0
		14.1892	0.791 751
		1.9666	0.321 87
		5.1477	1.0
		0.4962	1.0
		0.1533	1.0
		0.05	1.0
	p	18.1557	0.039 196
		3.9864	0.244 144
		1.1429	0.816 775
		0.3594	1.0
		0.1146	1.0
		0.03	1.0
	d	0.75	1.0
		0.133	1.0
N	s	5909.439 999	0.006 240
		887.451 000	0.047 669
		204.749 000	0.231 317
		59.837 600	0.788 869
		19.998 100	0.792 912
		2.686 000	0.323 609
		7.192 700	1.0
		0.7000	1.0
		0.2133	1.0
		0.07	1.0
	p	26.786	0.038 244
		5.9560	0.243 846
		1.7074	0.817 193
		0.5314	1.0
		0.1654	1.0
		0.05	1.0
	d	0.98	1.0
		0.133	1.0

[a]In Π symmetry we add two more p functions on each carbon and nitrogen atom with exponents: C—0.04,0.02; N—0.06,0.03. In Δ symmetry the following d functions were included on each carbon and nitrogen center with exponents: C—1.1,0.35,0.20,0.08,0.04; N—1.6,0.50,0.25,0.10,0.05. The coefficient for each function is 1.0.

remains finite and well defined). Several simplified schemes[1] have been suggested and applied satisfactorily to diatomic[30] and polyatomic[31] molecules, ranging from weakly polar to highly polar.

Differential cross sections for $J\rightarrow J'$ rotational transition were evaluated using the multipole-extracted adiabatic-nuclei (MEAN) approximation,[30] i.e.,

$$\frac{d\sigma}{d\Omega}(J\rightarrow J')=\frac{d\sigma^{\mathrm{FBA}}}{d\Omega}(J\rightarrow J') + \frac{k_{J'}}{4k_J}\sum_{l_t}[C(Jl_tJ';00)]^2 \times\frac{1}{k^2}\sum_{\lambda=0}^{\lambda_{\max}}(B_{\lambda,l_t}-B^{\mathrm{FBA}}_{\lambda,l_t})P_\lambda(\cos\theta)\ , \tag{1}$$

where the first term in (1) is the usual closed-form expression for the particular cross section in the laboratory-fixed coordinate frame (in the first Born approximation, FBA); k_J and $k_{J'}$ are, respectively, the wave vectors in the initial and the final channels; $C(\cdots)$ is a Clebsch-Gordan coefficient; and l_t is the angular momentum transferred during the collision. The B_{λ,l_t} are the expansion coefficients of the DCS, obtained from the scattering calculations, and $B^{\mathrm{FBA}}_{\lambda,l_t}$ are the corresponding quantities in the FBA, evaluated in the body-fixed coordinate frame with the fixed-nuclei approximation. The channel wave vectors k_J and $k_{J'}$ are related by

$$k_J^2-k_{J'}^2=B[J'(J'+1)-J(J+1)]\ , \tag{2}$$

where B is the rotational constant of the molecule (we took[25] $B=1.478\,22\ \mathrm{cm}^{-1}$).

The first and third terms in (1) distinguish the MEAN approximation from the normal adiabatic-nuclei approximation. They partially compensate for the essential flaw of the fixed-nuclei approximation by removing the high angular momentum contributions through cancellation between the second and third terms in (1). This is essential for $l_t=1$, for which $B_{\lambda,1}$ and $B^{\mathrm{FBA}}_{\lambda,1}$ individually diverge; it is also helpful for $l_t=2$, which brings in the long-range quadrupole moment and quadrupole polarizability interactions.

The coefficients B_{λ,l_t} and $B^{\mathrm{FBA}}_{\lambda,l_t}$ were evaluated for a series of electron energies (k^2 in the body-fixed coordinate frame) in the range 5×10^{-4} to 11.6 eV, and the final results obtained by interpolation of these coefficients on a natural cubic spline to any desired energy defined by (2) and the geometric mean $k^2=k_Jk_{J'}$. The MEAN approximation obviously fails very near threshold, but should be quite reliable at several times threshold. There have been no detailed evaluations for polar molecules, but a recent study[32] of the adiabatic-nuclei approximation for H_2 suggests that the accuracy of integrated cross sections exceeds 5% above twice threshold.

TABLE II. Properties of the HCN wave functions used in the present work and from measurements: E (total energy), I (ionization energy), D (dipole moment), Q (quadrupole moment). All quantities are in atomic units except I (eV).

	E	I	D	Q
Reference 21	−92.9147		1.264[a]	1.694[a]
Gaussian	−92.9015	13.85	1.267	1.772
Measured		13.91[b]	1.174[c]	2.3±0.5[d]

[a]Our results using this wave function.
[b]Reference 25.
[c]Reference 26.
[d]Reference 27.

III. NUMERICAL DETAILS

The ultimate accuracy of the results is a function of the precision of the numerical calculations as well as of the reliability of the physical model. The factor controlling the former in calculations such as this is the number of terms taken in several series and summations that affect the convergence of the results; many of these choices are described in this section. We strove for numerical precision of 5% or better in the most sensitive results, namely differential cross sections at small and large angles.

The number of terms taken in the expansion of the static electronic and nuclear interactions[33] were, respectively, at least 16 and 55 (the electronic term is small compared to the nuclear term beyond about 16 terms). In case of model exchange (the SE, SEP, and SEPO models), the number of expansion terms was taken to be the same as for the static electronic interaction, i.e., 16. For the ESE and ESEP models, we carried out convergence tests with respect to both the number of terms in the expansion and the radial extent of the functions. We found that 32, 20, and 10 terms ensure almost perfect convergence in Σ, Π, and Δ symmetries, respectively. Convergence with respect to the range of the exchange terms was tested at 12 and 16 a.u. for Σ and Π symmetries; they were found to converge to within 1%.

In order to extract reactance matrices from the scattering calculations, we matched to plane waves at a radius which depended both on the scattering energy and number of channels. The general criterion was about $10l/k$, where l is the order of the scattering expansion and k is the incident electron wave vector. Thus at the lower bound of the present energy regime (5×10^{-4} eV), we integrated up to a radial distance of about 24 700 a.u. for a 16-channel problem. This means that in all channels the contribution of the long-range dipole field has been accounted for completely.

The convergence of eigenphase sums was also tested for the lower symmetries (Σ and Π) with respect to the number of channels at various energies. In Σ symmetry and in the SE model we found that below 0.1 eV 16 channels ($l_c=15$) sufficed, and above this energy 28 channels ($l_c=27$), to achieve convergence in the eigenphase sums to within about 5%. A similar situation occurred in Π symmetry. For other models (ESEP, SEP, SEPO, etc.) the convergence properties of the calculations did not change significantly. In the ESE and ESEP models the convergence of the K matrix with respect to the expansion of the exchange potential has already been discussed.

Convergence of the eigenphase sums does not ensure convergence of differential and integral cross sections. In the evaluation of B_{λ,l_t} we used the l_t-reduced T matrices,[30]

$$T^{l_t}_{ll'}=\sum_m(-1)^m C(ll'l_t;m-m)T^m_{ll'}\ , \tag{3}$$

where m corresponds to the collision symmetry. We included T matrices for $m\le4$ (Σ, $m=0$; Π, $m=1$; Δ, $m=2$; ϕ, $m=3$; Γ, $m=4$) from the scattering calculations and for higher symmetries ($m>4$, $m\le l_c$) employed the unitarized Born approximation[34] (for $m>4$, calculated T matrices agreed with the unitarized Born values to within 1%). These were augmented by unitarized Born T matrices for $l_c<l\le l_b$, and for $l_t=1$ and 2 by FBA T matrices for $l_b<l\le l_{\max}$.

In order to determine l_b and $l_{\max}$, we must consider the λ sum in (1). For proper convergence, we require a large value of λ (say $\lambda_{\max}$). The criterion for choosing $\lambda_{\max}$ for $l_t=1$ and 2 was that $B_{\lambda,l_t}-B^{\rm FBA}_{\lambda,l_t}$ should vanish for $\lambda>\lambda_{\max}$. For $l_t=0$, $\lambda_{\max}$ was chosen large enough that the coefficients behaved as const/λ; the sum from $\lambda_{\max}+1$ to ∞ was evaluated in a closed form. For $l_t=0$, 1, and 2, proper convergence in the DCS dictated the choices $\lambda_{\max}=40$, 40, and 30, respectively; for $l_t>2$, 20 λ's was sufficient. We included all $l_t\le7$ in evaluating (1). One should note that the calculation of integral cross sections requires only the $\lambda=0$ component and the momentum-transfer cross sections only $\lambda=0$ and 1. This part of the calculation can be done very quickly with almost perfect convergence. As a general rule, good convergence requires $l_b\gtrsim2\lambda_{\max}$; we took $l_b=80$ for all l_t. For $l_t=1$ and 2 this determines $l_{\max}$ ($=l_b+\lambda_{\max}$), since the FBA is assumed valid and hence the contributions to the sum in (1) cancel identically for higher angular momenta. For $l_t=0$ and $l_t\ge3$ we took $l_{\max}=l_b$.

We used experimental values of the dipole moment and the polarizability in the first term of (1) in order to partially correct for the errors in the Hartree-Fock (or the Gaussian) basis functions. However, due to large uncertainty involved in the experimental value of the quadrupole moment (2.3±0.5 a.u.), we thought it better to make use of our calculated value, i.e., 1.772 a.u., in the first term in (1). Since calculated values from the employed

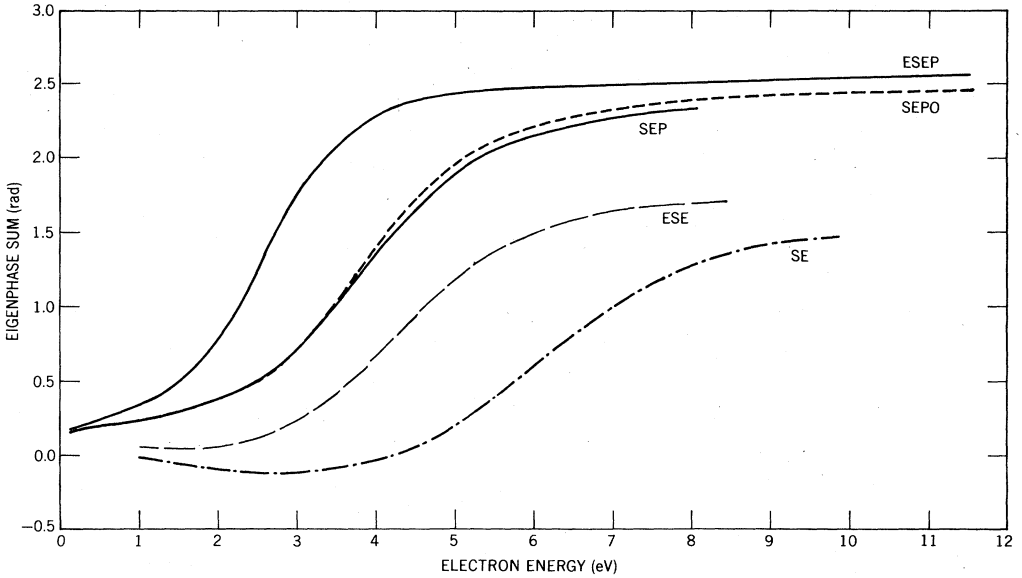

FIG. 2. Eigenphase sum for Π-symmetry scattering of electrons by HCN. For notation see the text.

wave functions are implicit in the second term in (1), they were also used in the third term.

IV. RESULTS AND DISCUSSION

In Fig. 2 we have plotted the Π-symmetry eigenphase sums (0.1—11.6 eV) from the SE, ESE, SEP, SEPO, and ESEP models. There is clearly a resonance around 2.6 eV in the ESEP model.[35] The position and width of this Π resonance are given in Table III for various models. The model-exchange curves (with and without orthogonalization) differ significantly from the exact-exchange curves. However, the effect of orthogonalization is small (less than 5%) in this symmetry. Polarization also has a significant effect on the position and width of the resonance.

In Fig. 3 the eigenphase sums in the Σ and the Δ symmetries are shown. Orthogonalization is important in Σ symmetry in the model-exchange case. The difference between the ESEP and the SEPO models is much smaller than in Π symmetry, but polarization effects are still very important. There is no evidence of any resonance structure in Σ symmetry at equilibrium geometry. The ESEP and SEPO Δ eigenphase sums differ by less than 15% at all energies.

It is interesting to compare the ESEP Π resonance with the experimental transmission curve of Burrow.[12] Burrow has measured the derivative of the transmitted electron current through HCN and observed a resonance around 2.26 eV. These measurements were taken with weak rejection and therefore the effect of forward scattering (dipole scattering) was excluded in the derivative spectra. We therefore compare our momentum-transfer cross section (first derivative) with Burrow's result in Fig. 4. The agreement is striking except that the position is shifted toward a higher energy (from 2.26 to 2.56 eV). Despite the excellent agreement in the apparent (peak-to-peak) width (~1.3 eV) of the two curves (Fig. 4), our calculated Π-resonance width is about 1.8 eV (Table III). This large difference is due to the background effects.

In another experimental observation,[13] for vibrational excitation of HCN, preliminary results show a broad

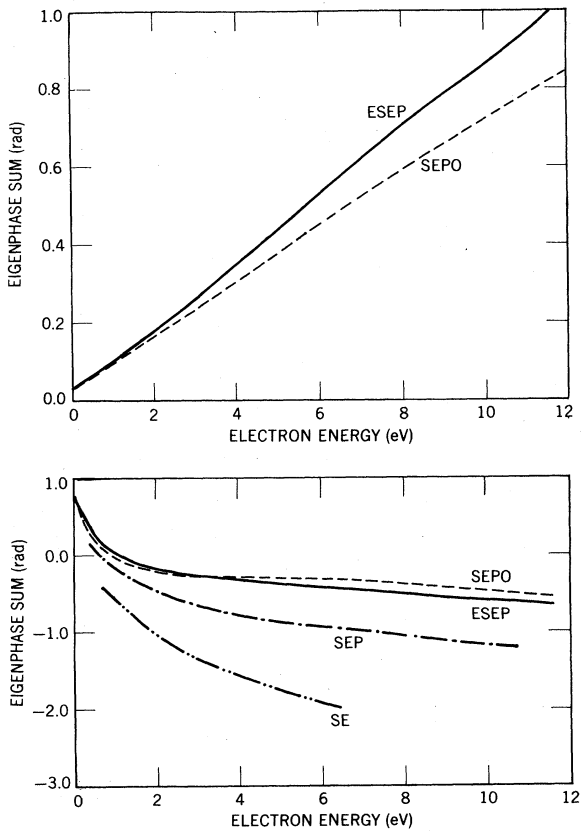

FIG. 3. Eigenphase sums for Σ- (lower set) and Δ- (upper set) symmetry scattering of electrons by HCN. For notation see the text.

TABLE III. Resonance parameters in various models in the Π symmetry of *e*-HCN scattering (in eV).

	Position	Width
ESEP[a]	2.56	1.78
ESEP[b]	2.71	1.91
SEPO or SEP	3.80	2.40
ESE	4.30	3.10
SE	6.10	3.90
Expt.	2.26,[c] 2.3[d]	

[a]Using Eq. (6) of Ref. 28 for the correlation-polarization potential.
[b]Using Eq. (9) of Ref. 28 for the correlation-polarization potential.
[c]Reference 12.
[d]Reference 13.

shape resonance around 2.3 eV, which was deduced to be Π as the ν_3 CN stretching and ν_2 bending modes are excited [such a conclusion follows earlier study of the isoelectronic C_2H_2 molecule, where the C_2H^- fragment is formed

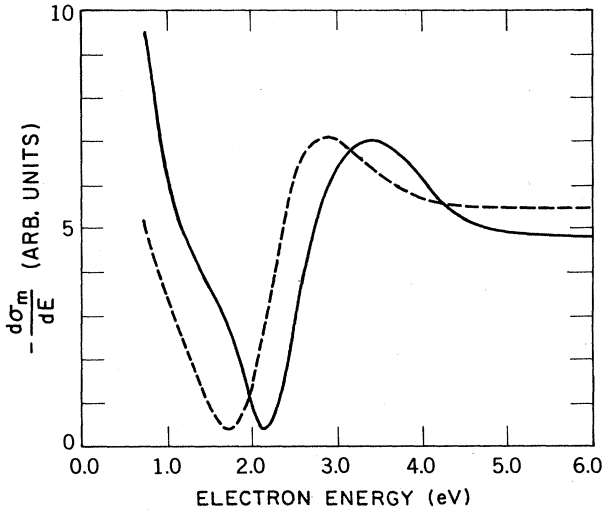

FIG. 4. $d\sigma_m/dE$ (σ_m is the momentum-transfer cross section and E is the electron energy) vs derivative of the transmitted current for *e*-HCN elastic scattering: ——, present derivative; – – – –, experimental curve (Ref. 12).

TABLE IV. Partial integral cross sections at some selected energies for *e*-HCN scattering (in units of a_0^2).

Energy (eV)	$J \rightarrow J'$	ESEP (Present)	Saha *et al.*[a]	UTDP[b]	FBA (Present)
0.001	0→1	1.61(5)[c]	1.19(5)	2.25(5)	3.42(5)
	0→2				
	1→2				1.20(5)
0.003	0→1	1.09(5)	1.33(5)	1.67(5)	2.34(5)
	0→2	7.79(3)	5.39(3)		2.94
	1→2	4.80(4)	6.20(4)	7.86(4)	9.29(4)
0.005	0→1	7.67(4)	8.49(4)	9.57(4)	1.25(5)
	0→2	3.90(3)	4.00(3)		3.33
	1→2	3.57(4)	4.16(4)	5.14(4)	6.76(4)
0.007	0→1	6.79(4)	7.29(4)	8.45(4)	9.67(4)
	0→2	2.60(3)	3.51(3)		3.51
	1→2	3.46(3)	3.85(4)	4.59(4)	5.37(4)
0.01	0→1	5.17(4)	5.49(4)	5.88(4)	7.34(4)
	0→2	1.82(3)	2.38(3)		3.67
	1→2	2.71(3)	2.96(4)	3.27(4)	4.15(4)
0.03	0→1	2.27(4)	2.16(4)	2.54(4)	3.03(4)
	0→2	7.88(2)	9.39(2)		4.16
	1→2	1.27(4)	1.37(4)	1.46(4)	1.78(4)
0.05	0→1	1.53(4)	1.32(4)	1.68(4)	1.98(4)
	0→2	5.50(2)	5.86(2)		4.35
	1→2	8.74(3)	8.74(3)	9.82(3)	1.17(4)
0.10	0→1	8.79(3)	6.69(3)	9.51(3)	1.10(4)
	0→2	3.20(2)	2.89(2)		4.78
	1→2	5.15(3)	4.55(3)	5.63(3)	6.60(3)

[a]Reference 2.
[b]Unitarized-time-dependent-perturbation theory (Ref. 37), as calculated in Ref. 2.
[c]The numbers in parentheses are the powers of ten by which the number is multiplied.

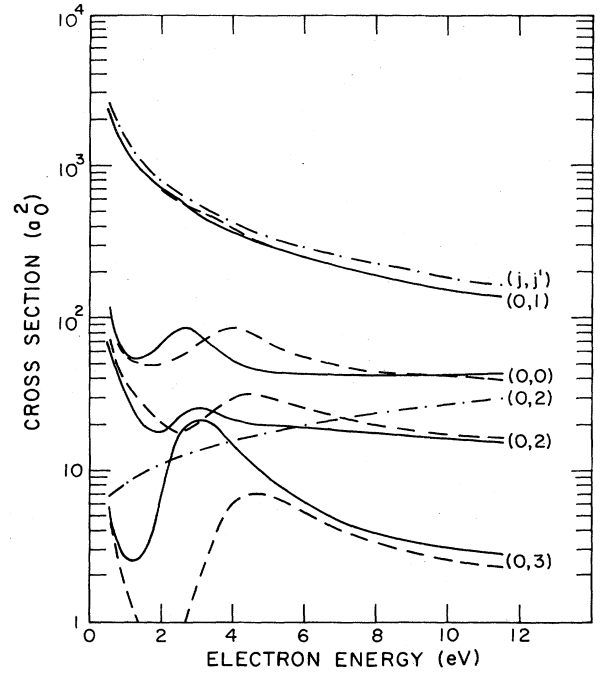

FIG. 5. Partial integrated cross sections for various rotational transitions in e-HCN scattering: ESEP (——), SEPO (– – – –), FBA (—·—·—).

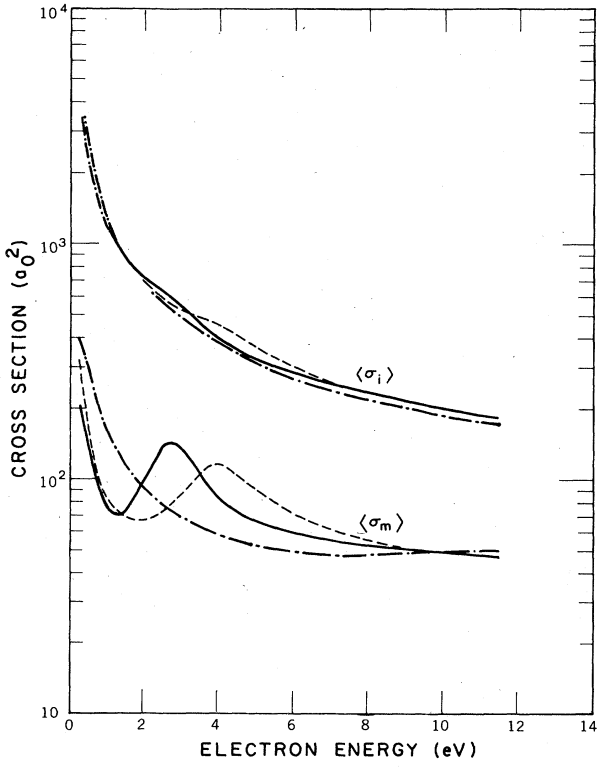

FIG. 6. Rotationally summed integrated and momentum-transfer cross sections (thermally averaged at 320 K) for e-HCN: ESEP (——), SEPO (– – – –), FBA (—·—·—).

through a $^2\Pi$ shape resonance around 2.3 eV when this state correlates with $H^- + C_2H(^2\Pi)$ at 3.15 eV]. A study of dissociative attachment in HCN also showed a CN^- peak at about 2.5 eV.[11]

Assuming that the Π resonance obtained in the present work is the same feature observed in the three measurements,[11–13] we must seek an explanation for our result being ~0.4 eV too high. The MEAN approximation is unlikely to be at fault so far above the vibrational and rotational thresholds, and the polarization-correlation model yielded much better results for the position and width of the N_2 Π_g resonance.[28,36] The most likely explanation[12,13] is that the resonance state of HCN^- is actually bent, leading to a significant reduction in its energy; stretching of either bond would be less likely to result in such a substantial effect.

The above hypothesis would also help explain the observed[11] large CN^- production in e-HCN dissociative attachment. A Π resonance would not ordinarily couple strongly to the final state of this reaction, which is Σ. Significant bending would break the symmetry of the linear geometry. As noted, we obtained no evidence of a Σ resonance in the energy range 0–12 eV in linear geometry. The 6.2-eV resonance observed by Tronc[11] may well be the state studied by Pacansky *et al.*,[15] as both the measurement and calculation indicated significant σ char-

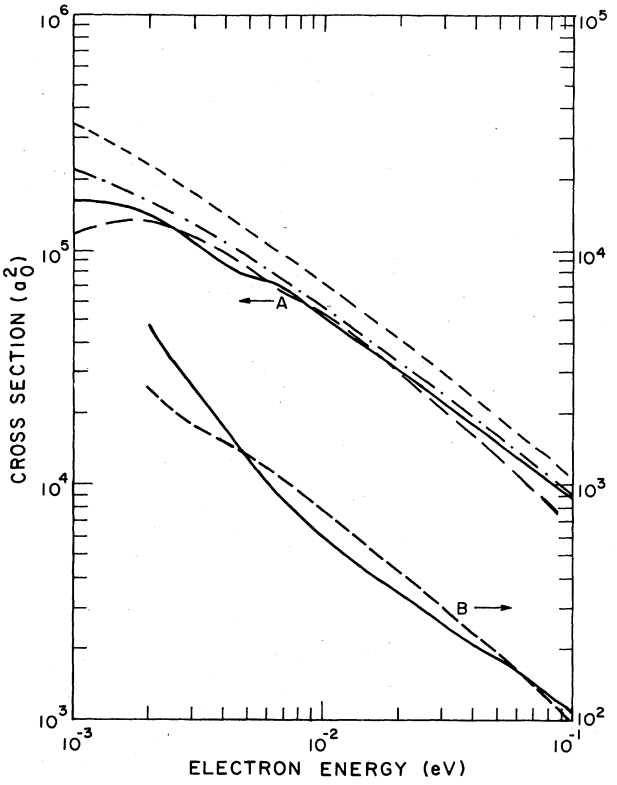

FIG. 7. Rotational excitation cross sections for e-HCN scattering: ESEP or SEPO (——), FBA (– – – –), Saha *et al.* (Ref. 2) (– – – –), UTDP (—·—). The sets of curves *A* and *B* (divided by a factor of 3) are for 0→1 and 0→2 transitions, respectively.

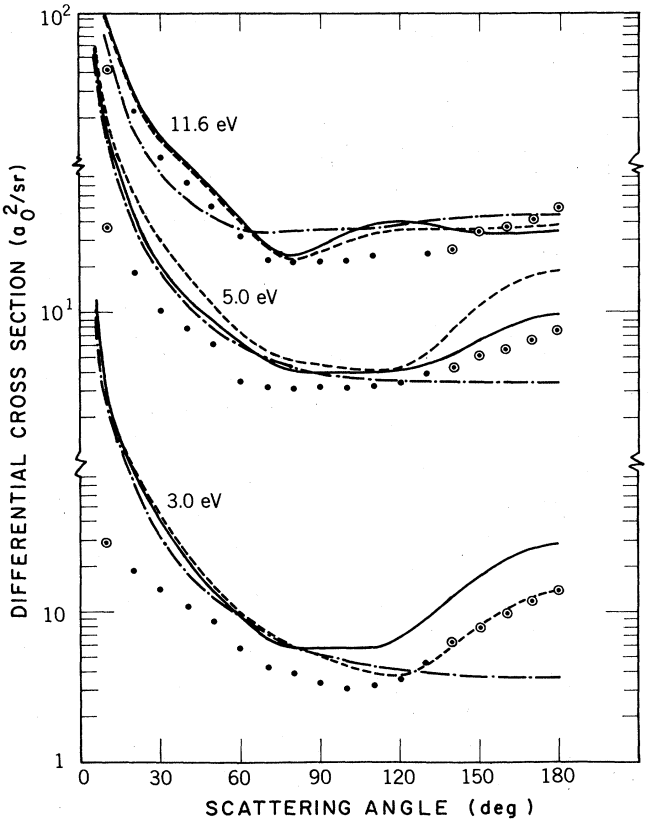

FIG. 8. Differential cross sections for vibrationally elastic scattering (rotationally summed) of electrons by HCN. Present calculations: ESEP (——), SEPO (– – – –), FBA (—·—). Experimental data (●) are due to Srivastava *et al.* (Ref. 9) (the ⊙ are extrapolated points).

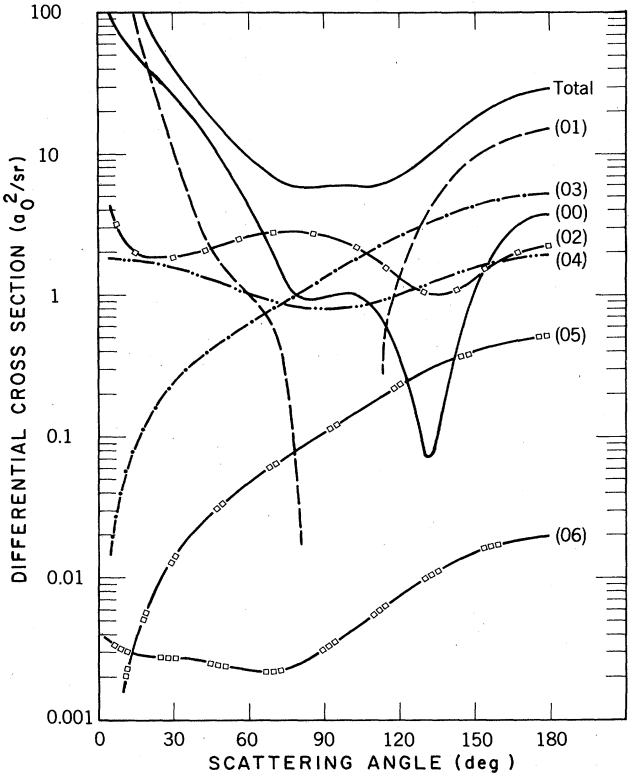

FIG. 9. Differential cross sections for various rotational excitations ($J - J'$) in HCN by electron impact at 3 eV.

acter in the unpaired electron.

In Fig. 5 the partial integral cross sections from $J=0$ to $J'=0$–3 from the ESEP and SEPO models are plotted. The main difference between the two models is the shift of the 2.6-eV resonance to about 4 eV in the SEPO model. Except for the 0→1 transition, all the transitions exhibit this structure clearly around 2.6 eV (4.0 eV in SEPO). We know of no experimental or theoretical data with which to compare our results in this energy range.

In Fig. 6 the thermally averaged (at 320 K) integral ($\langle\sigma_i\rangle$) and momentum-transfer ($\langle\sigma_m\rangle$) cross sections are illustrated for both the ESEP and SEPO models, along with FBA results. The Π structure is quite distinct in the $\langle\sigma_m\rangle$ curves from both models, while in the $\langle\sigma_i\rangle$ curve this feature is suppressed due to dominant dipole forward scattering. Since the FBA is quite reasonable for the dipole scattering, the $\langle\sigma_i\rangle$ FBA curve is in quite close agreement with the ESEP or SEPO curves. The $\langle\sigma_m\rangle$ FBA curve does not, however, reproduce any feature in the calculated cross section. There are no data available in this range for either $\langle\sigma_m\rangle$ or $\langle\sigma_i\rangle$ except one measurement for $\langle\sigma_m\rangle$ at 25 meV by Tice and Kivelson:[10] Our $\langle\sigma_m\rangle$ value, $6.95\times10^3 a_0^2$ at 25 meV (ESEP model), agrees quite closely with their experimental value of $7.88\times10^3 a_0^2$.

In a very low energy region (6×10^{-4} to 0.1 eV), Saha *et al.*[2] carried out laboratory-frame close-coupling calculations for *e*-HCN scattering for the partial (dipole and quadrupole) integral cross sections. In their calculation they employed dipole, quadrupole, and polarization potentials with the assumption of a repulsive potential wall for values of radial distance r less than the molecular dimension. We compare our numbers with theirs for the transitions 0→1, 0→2, and 1→2 in Table IV. Also shown in this table are the results in the unitarized-time-dependent-perturbation (UTDP) theory[37] and the FBA. The same data are also plotted in Fig. 7. In this energy range our SEPO and ESEP results do not differ significantly, so that we have shown only ESEP cross sections in Table IV and Fig. 7. The difference between the present and the Saha *et al.* calculations is within 25% and 30% for 0→1 and 0→2 transitions, respectively, in the whole energy region. This disagreement is indicative of the importance of short-range interactions and exchange effects. The difference in the 0→2 curves is also due to different

TABLE V. Integral (σ_I) and momentum-transfer (σ_m) cross sections for *e*-HCN elastic scattering (in units of 10^{-16} cm^2).

Energy (eV)	σ_I Present	σ_I Expt.[a]	σ_m Present	σ_m Expt.[a]
3	148.3	23.0	37.0	18.0
5	89.63	18.0	18.55	14.0
11.6	50.4	16.0	13.10	9.7

[a]Reference 9.

values of the quadrupole moment used in the two calculations. The UTDP and the FBA results are too high throughout.

In Fig. 8 we plot our DCS at 3, 5, and 11.6 eV and compare them with experimental results.[9] It is clear from this figure that the ESEP results are qualitatively in agreement (as compared to SEPO results) with the experiment. Quantitatively, however, our ESEP results are larger by roughly a factor of 2 at 3 eV. At small angles ($\theta \leq 20°$) the measured results are flatter at all energies. This leads to very large differences in total and momentum-transfer cross sections (Table V), which were obtained from the measurements by extrapolating the data to small and large angles.

In order to see the contribution of individual transitions to the total differential cross sections, we show partial DCS's from $J=0$ to $J'=0$–6 in Fig. 9. There are sharp dips around 90° in the $0\rightarrow 1$ transition and around 130° in the elastic ($0\rightarrow 0$) transition; the contributions from other transitions ($0\rightarrow 2$, $0\rightarrow 3$, $0\rightarrow 4$, $0\rightarrow 5$) suppress these dips in the total DCS curve. It seems that no individual excitation dominates the total DCS curve except at very low angles ($\theta \leq 10°$), which is mainly due to the $0\rightarrow 1$ transition.

V. SUMMARY AND CONCLUSIONS

We studied vibrationally and electronically elastic e-HCN scattering in the range 6×10^{-4} to 11.6 eV. Two models were employed, namely ESEP and SEPO, the only difference between the two being that in the ESEP exchange has been treated exactly, while in the SEPO a model potential was employed along with the orthogonalization procedure. At low energies ($E \leq 0.5$ eV) the SEPO and ESEP models yield nearly identical results, but a dramatic difference appears in the resonant region. The 3.8-eV SEPO Π resonance is shifted toward the experimentally observed position for the ESEP model. Since our calculations involve no adjustable parameters, the good agreement between the experimental and the present ESEP resonance parameters is quite satisfying; with the inclusion of zero-point averaging over bending much better results might be expected. Study of the scattering behavior, particularly in resonant symmetries, as a function of deviations from linear equilibrium geometry is in progress. Due to the large difference between the present total DCS and the measurements of Srivastava *et al.*,[9] more experimental study of the reaction is suggested.

ACKNOWLEDGMENTS

This work was supported by the U.S. Department of Energy (Office of Basic Energy Sciences). We gratefully acknowledge very useful discussions with Paul Burrow and Nely T. Padial and thank Dr. M. Tronc for permission to cite his results in advance of publication.

---

*Present address: Department of Chemistry, The Ohio State University, 140 West 18th Ave., Columbus, OH 43210.
†Quantum Physics Division, National Bureau of Standards.

[1]Y. Itikawa, Phys. Rep. **46**, 117 (1978); N. F. Lane, Rev. Mod. Phys. **52**, 29 (1980); D. W. Norcross and L. A. Collins, Adv. A. Mol. Phys. **18**, 341 (1982); a more recent summary on e-molecule scattering can be found in *Electron-Molecule Interactions and Their Applications,* edited by L. G. Christophorou (Academic, New York, 1984), Vol. 1.
[2]S. Saha, S. Ray, B. Bhattacharya, and A. K. Barua, Phys. Rev. A **23**, 2926 (1981).
[3]P. Seal, Indian J. Phys. **54B**, 504 (1980).
[4]I. I. Fabrikant, Phys. Lett. **77A**, 421 (1980); J. Phys. B **16**, 1253 (1983).
[5]A. Jain and S. S. Tayal, J. Phys. B **17**, L37 (1984).
[6]C. R. Quick, C. Wittig, and J. B. Laudenslager, Opt. Commun. **18**, 268 (1976).
[7]D. M. Rank, C. H. Townes, and W. J. Welch, Science **174**, 1083 (1971); S. Green and P. Thaddeus, Astrophys. J. **191**, 653 (1974).
[8]A. S. Dickinson, T. G. Phillips, P. F. Goldsmith, I. C. Percival, and D. Richards, Astron. Astrophys. **54**, 645 (1977); see also M. Openheimer and A. Dalgarno, Astrophys. J. **192**, 29 (1974).
[9]S. K. Srivastava, H. Tanaka, and A. Chutjian, J. Chem. Phys. **69**, 1493 (1978); S. Trajmar, D. F. Register, and A. Chutjian, Phys. Rep. **97**, 219 (1983).
[10]R. Tice and D. Kivelson, J. Chem. Phys. **46**, 4748 (1967).
[11]M. Inoue, J. Chim. Phys. **63**, 1061 (1966).
[12]P. D. Burrow (private communication); see also L. Ng, U. Balaji, and K. D. Jordan, Chem. Phys. Lett. **101**, 171 (1983).
[13]M. Tronc (private communication).
[14]See citations in Ref. 15.
[15]J. Pacansky, N. S. Dalal, and P. S. Bagus, Chem. Phys. **32**, 183 (1978).
[16]W. R. Garrett, Chem. Phys. Lett. **62**, 325 (1979).
[17]See N. T. Padial, D. W. Norcross, and L. A. Collins, Phys. Rev. A **27**, 141 (1983); N. T. Padial and D. W. Norcross, *ibid.* **29**, 1590 (1984).
[18]M. A. Morrison, N. F. Lane, and L. A. Collins, Phys. Rev. A **15**, 2186 (1977); M. A. Morrison and L. A. Collins, *ibid.* **17**, 918 (1978).
[19]N. T. Padial and D. W. Norcross (unpublished).
[20]B. I. Schneider and L. A. Collins, Phys. Rev. A **24**, 1264 (1981); T. N. Rescigno and A. E. Orel, *ibid.* **24**, 1267 (1981).
[21]A. D. McLean and M. Yoshimine, *Tables of Linear Molecule Wave Functions* [IBM J. Res. Dev. **12**, 206 (1968), supplement].
[22]M. H. Mittleman and S. T. Watson, Ann. Phys. (N.Y.) **10**, 268 (1960); S. Hara, J. Phys. Soc. Jpn. **22**, 710 (1967).
[23]F. W. Bobrowicz and W. A. Goddard, in *Methods of Electronic Structure,* edited by H. F. Schaefer (Plenum, New York, 1977), Vol. 3, p. 77.
[24]L. A. Collins and B. I. Schneider (private communication).
[25]G. Herzberg, *Electronic Spectra of Polyatomic Molecules* (Van Nostrand, New York, 1966).

[26]A. L. McClellan, *Tables of Experimental Dipole Moments* (Freeman, San Francisco, 1963); see also R. L. Deleon and J. S. Muenter, J. Chem. Phys. **80**, 3992 (1984).

[27]S. L. Hartford, W. C. Allen, C. L. Norris, E. F. Pearson, and W. H. Flygare, Chem. Phys. Lett. **18**, 153 (1973).

[28]J. O'Connell and N. F. Lane, Phys. Rev. A **27**, 1893 (1983); N. T. Padial and D. W. Norcross, Phys. Rev. A **29**, 1742 (1984).

[29]*Molekeln I (Kerngerüst),* Vol. 1, Part 2 of *Landolt-Börnstein,* edited by A. Eucken and K. H. Hellwege (Springer, Berlin, 1951).

[30]D. W. Norcross and N. T. Padial, Phys. Rev. A **25**, 226 (1982).

[31]A. Jain and D. G. Thompson, J. Phys. B **15**, L631 (1982); **16**, 2593 (1983); **16**, 3077 (1983); **17**, 460 (1984).

[32]M. A. Morrison, A. N. Feldt, and D. Austin, Phys. Rev. A **29**, 2518 (1984).

[33]M. A. Morrison, Comput. Phys. Commun. **21**, 63 (1980); G. B. Schmid and D. W. Norcross, Comput. Phys. Commun. **21**, 79 (1980).

[34]N. T. Padial, D. W. Norcross, and L. A. Collins, J. Phys. B **14**, 2901 (1981).

[35]Except for the second line in Table III, all results reported in this paper are based on the use of Eq. (6) of Ref. 28 for the correlation-polarization potential. While Eq. (9) of Ref. 28 is presumably more accurate, only the position and width of the II resonance were substantially affected.

[36]In unpublished work we also obtained very satisfying results from this model (ESEP) for the e-CO II resonance ($E_r = 1.85$ eV, $\Gamma = 0.95$ eV) compared with the experimental position and width of 1.8—1.9 eV and ~ 1.0 eV, respectively [M. Tronc, R. Azria, and Y. Le Coat, J. Phys. B **13**, 2327 (1980)].

[37]A. S. Dickinson and D. Richards, J. Phys. B **8**, 2846 (1975).